Gulf Journal of Mathematics
Vol 20, Issue 2 (2025) 175-193

ISSN: 2309-4966
https://doi.org/10.56947/gjom.v20i2.3189

WELL-POSEDNESS AND FINITE VOLUME APPROXIMATION OF ELASTIC-ELASTIC INTERACTION MODEL WITH JUMP EMBEDDED BOUNDARY CONDITIONS

AHMED AYOUB BOUKELIA[1*] and MOHAMED KARA[1]

Abstract. This paper addresses an elastic–elastic interaction problem governed by jump-embedded boundary conditions (J.E.B.C.) on the interface between two subdomains, based on the fictitious domain principle. We develop a variational formulation and prove the existence and uniqueness of weak solutions using the Lax–Milgram theorem. A penalized problem is introduced to approximate spring-law-type interface conditions, and strong convergence is established, with error estimates explicitly depending on the positive penalization parameter. A finite volume discretization is proposed, preserving local conservation in interior control volumes (CVs), while treating interface CVs separately due to the jump conditions. Numerical experiments demonstrate convergence rates between first and second order under various interface conditions, confirming the theoretical results. The proposed framework provides a reliable foundation for further developments in elasticity interface modeling.

Keywords. Existence and uniqueness, Finite volume method, Interaction conditions, Linear elasticity, Numerical simulation.
2020 Mathematics Subject Classification. 35D30, 35A01, 74B05, 74-XX.

1. Introduction

Elastic interactions between multiple materials or components are central to a wide range of physical and engineering systems, including biomechanics, geomechanics, and composite structures. In many such systems, distinct elastic subdomains interact across interfaces where discontinuities in displacement or stress naturally arise. Accurately capturing these discontinuities poses substantial mathematical and numerical challenges.

The well-posedness of mathematical models for the Stokes / Brinkman problem with J.E.B.C. at fluid-porous interfaces has been rigorously analyzed in [1, 2], including the Whitaker–Ochoa-Tapia and Beavers–Joseph interface conditions. These works focus on fluid–porous interaction problems and provide a unified variational framework for various physically relevant interface conditions. In contrast, the treatment of linear elasticity problems involving an elastic medium

Date: Received: Jun 26, 2025; Accepted: Jul 27, 2025.
* Corresponding author

coupled with an extended domain through J.E.B.C. has been addressed using fictitious domain approaches in [8, 9, 7], extending the methodology to elasticity interfaces.

In this paper, we investigate the well-posedness of an elastic–elastic interaction problem governed by jump-embedded boundary conditions. We then study the asymptotic convergence of the model toward an elastic–elastic transmission problem with spring-type interface conditions. We begin by formulating the variational problem and establishing its well-posedness using classical tools from functional analysis. The analysis is then extended to special cases, such as the spring-law interface and its penalized approximation, for which we demonstrate strong convergence and derive *a priori* error estimates.

To address the computational aspects of our framework, we develop a finite volume method (FVM) specifically tailored to this class of problems, drawing on established techniques [5, 3, 4]. Our FVM implementation offers three key advantages: first, strict enforcement of local conservation laws; second, robust handling of complex interface geometries; and third, a unified approach to various transmission conditions.

We validate our approach through extensive numerical experiments examining vertical, L-shaped, and rectangular interface configurations, which collectively demonstrate the method's accuracy and convergence properties under systematic grid refinement.

The novelty of this work is that, to the best of our knowledge, it is the first to rigorously establish the well-posedness and convergence analysis of elastic–elastic interaction models governed by J.E.B.C., combined with a finite volume discretization specifically designed to ensure local conservation and accurately handle complex interface geometries. This new framework generalizes existing fictitious domain approaches beyond fluid–porous systems to purely elastic coupled problems with discontinuous interface conditions.

The remainder of this work is organized as follows. Section 2 establishes the well-posedness of our elastic–elastic model with J.E.B.C.. Section 3 introduces the spring-law-type interface conditions, while Section 4 provides a rigorous convergence analysis from the J.E.B.C. model to the spring-law formulation. Section 5 details our finite volume discretization methodology, and Section 6 presents comprehensive numerical validation across different domain configurations. We conclude with a summary of key findings and a discussion of promising future research directions, particularly regarding extensions to nonlinear and dynamic problems.

2. A well-posed elastic–elastic problem with jump embedded boundary conditions

We work on the composite region

$$\Omega = \Omega_1 \cup \Sigma \cup \Omega_2,$$

where Ω_1 and Ω_2 are two subdomains joined along the interface Σ. For each $i \in \{1, 2\}$, let

$$\Gamma_i = \partial\overline{\Omega}_i \setminus \Sigma$$

be the portion of $\partial\Omega_i$ not lying on Σ. We denote by ν the normal outward unit vector on $\partial\Omega$, and by n the normal outward unit vector on the interface Σ, oriented from Ω_1 into Ω_2.

For $i = 1, 2$, let $\sigma_i(u_i) = \mathbb{C}_i : \varepsilon(u_i)$ denote the Cauchy stress tensor in the linear elasticity domain Ω_i, where u_i is the displacement field, $\varepsilon(u_i) = \frac{1}{2}(\nabla u_i + \nabla u_i^\top)$ is the infinitesimal strain tensor, and $\mathbb{C}_i$ is the fourth-order elasticity tensor, assumed to be symmetric and uniformly elliptic. The elastic–elastic transmission problem with jump-embedded boundary conditions, based on a fictitious domain approach, is posed on the interface Σ and reads:

$$-\nabla \cdot \sigma_1(u) = f_1 \quad \text{in } \Omega_1, \tag{2.1}$$

$$-\nabla \cdot \sigma_2(u) = f_2 \quad \text{in } \Omega_2, \tag{2.2}$$

$$u = 0 \quad \text{on } \Gamma_1 \cup \Gamma_2, \tag{2.3}$$

$$[\![\sigma(u) \cdot n]\!]_\Sigma = M\overline{u}|_\Sigma - g \quad \text{on } \Sigma, \tag{2.4}$$

$$\overline{\sigma(u) \cdot n}|_\Sigma = S[\![u]\!]_\Sigma - h \quad \text{on } \Sigma, \tag{2.5}$$

with $f_i \in L^2(\Omega_i)^d$ and $u|_{\Omega_i} = u_i$ for $i = 1, 2$.

The jump and the arithmetic mean over Σ are defined as follows:

$$[\![u]\!]_\Sigma = u_2|_\Sigma - u_1|_\Sigma, \qquad [\![\sigma(u) \cdot n]\!]_\Sigma = \sigma_2(u_2) \cdot n - \sigma_1(u_1) \cdot n,$$
$$\overline{u}|_\Sigma = (u_2|_\Sigma + u_1|_\Sigma)/2, \quad \overline{\sigma(u) \cdot n}|_\Sigma = (\sigma_1(u_1) \cdot n + \sigma_2(u_2) \cdot n)/2.$$

The functions $g, h \in H^{1/2}(\Sigma)^d$ represent interface force terms and $M(x), S(x) \in \mathbb{R}^{d\times d}$ are $\mathbb{L}^\infty$ measurable functions with symmetric matrix values. These, together with $\mathbb{C}_1$ and $\mathbb{C}_2$, are assumed to satisfy the following ellipticity conditions: for $i = 1, 2$, let $\alpha_1, \alpha_2, M_0, S_0 > 0$ be constants such that

$$\mathbb{C}_i \in \mathbb{L}^\infty(\Omega_i)^{d\times d} \text{ and } \mathbb{C}_i(x)\xi : \xi \geq \alpha_i|\xi|^2, \quad \text{a.e. in } \Omega_i, \quad \forall \xi \in \mathbb{R}^{d\times d}, \tag{A1}$$

$$M(x)\xi \cdot \xi \geq M_0|\xi|^2, \quad S(x)\xi \cdot \xi \geq S_0|\xi|^2, \quad \text{a.e. on } \Sigma, \quad \forall \xi \in \mathbb{R}^d, \tag{A2}$$

where $|\cdot|$ denotes the Frobenius norm.

Remark 2.1. Throughout the paper, we denote by u the global displacement field defined in the union domain $\Omega = \Omega_1 \cup \Omega_2$, such that

$$u|_{\Omega_1} = u_1, \qquad u|_{\Omega_2} = u_2.$$

For notational convenience, we write u without subscripts and interpret it piecewise on each subdomain. Similarly, all expressions involving u, such as ∇u, $\varepsilon(u)$, and the bilinear form $a(u, w)$, are to be understood as acting separately on Ω_1 and Ω_2, with appropriate traces defined on the interface Σ.

Weak Formulation: The functional space required for the weak formulation is introduced below

$$W \equiv \{w \in L^2(\Omega)^d : w|_{\Omega_1} \in H^1_{0,\Gamma_1}(\Omega_1)^d,\ w|_{\Omega_2} \in H^1_{0,\Gamma_2}(\Omega_2)^d\},$$

with the norm:

$$\|w\|_W^2 = \|\nabla w\|^2_{0,\Omega_1} + \|\nabla w\|^2_{0,\Omega_2}.$$

Hence, the variational formulation becomes: Find $u \in W$ such that for all $w \in W$,

$$a(u, w) = \ell(w), \tag{2.6}$$

with

$$a(u, w) = \int_{\Omega_1} \mathbb{C}_1 \varepsilon(u) : \varepsilon(w)\, dx + \int_{\Omega_2} \mathbb{C}_2 \varepsilon(u) : \varepsilon(w)\, dx$$
$$+ \int_\Sigma M \overline{u}|_\Sigma \cdot \overline{w}|_\Sigma\, ds + \int_\Sigma S[\![u]\!]_\Sigma \cdot [\![w]\!]_\Sigma\, ds,$$

and

$$\ell(w) = \int_\Omega f \cdot w\, dx + \int_\Sigma g \cdot \overline{w}|_\Sigma\, ds + \int_\Sigma h \cdot [\![w]\!]_\Sigma\, ds,$$

where $\int_\Omega f \cdot w\, dx = \int_{\Omega_1} f_1 \cdot w\, dx + \int_{\Omega_2} f_2 \cdot w\, dx$.

Before we proceed with the solvability theorem, we state the following result, which will be used in its proof.

Proposition 2.2. *Let $u \in H^1(\Omega)^d$, and define*

$$\varepsilon(u) \;=\; \frac{1}{2}\big(\nabla u + (\nabla u)^\top\big)$$

as the symmetric gradient of u. Then the following estimate holds:

$$\|\varepsilon(u)\|_{L^2(\Omega)} \;\leq\; \|\nabla u\|_{L^2(\Omega)}. \tag{2.7}$$

Proof. For each $x \in \Omega$, we write:

$$\nabla u = \varepsilon(u) + \omega(u), \quad \text{with } \omega(u) := (\nabla u - \nabla u^\top)/2,$$

so that $\varepsilon(u)$ is symmetric and $\omega(u)$ is skew-symmetric. The Frobenius inner product of these two matrices vanishes:

$$\langle \varepsilon(u), \omega(u) \rangle = 0,$$

and therefore, by the Pythagorean identity for matrices,

$$|\nabla u|^2 = |\varepsilon(u)|^2 + |\omega(u)|^2 \geq |\varepsilon(u)|^2.$$

Integrating over Ω taking square roots yields the desired inequality. □

Now, we present the following global solvability theorem.

Theorem 2.3 (Global Solvability of the Elastic/Elastic Model with J.E.B.C.)**.** *Let the volume forces $f_i \in L^2(\Omega_i)^d$ for $i = 1, 2$, and let the interface forces $g, h \in H^{1/2}(\Sigma)^d$. If $\mathbb{C}_1$, $\mathbb{C}_2$, M, and S satisfy the assumptions (A1)–(A2), then the problem (2.1)–(2.5) admits a **unique weak solution** $u \in W$ that satisfies the variational formulation (2.6).*

In addition, there exists a constant $C > 0$, depending only on the structural parameters (but not on the data), for which the following bound holds:

$$\|u\|_W \leq C \left(\|f\|_{0,\Omega} + \|h\|_{1/2,\Sigma} + \|g\|_{1/2,\Sigma} \right).$$

Proof. **Coercivity of $a(\cdot,\cdot)$:** Let $u \in W$. The bilinear form gives:

$$a(u,u) = \int_{\Omega_1} \mathbb{C}_1 \varepsilon(u) : \varepsilon(u)\, dx + \int_{\Omega_2} \mathbb{C}_2 \varepsilon(u) : \varepsilon(u)\, dx$$
$$+ \int_{\Sigma} M \overline{u}|_\Sigma \cdot \overline{u}|_\Sigma \, ds + \int_\Sigma S [\![u]\!]_\Sigma \cdot [\![u]\!]_\Sigma \, ds.$$

From the uniform ellipticity assumption (A1) and by applying Korn's inequality on each subdomain Ω_i, we obtain, for $i = 1, 2$,

$$\int_{\Omega_i} \mathbb{C}_i \varepsilon(u) : \varepsilon(u)\, dx \geq \alpha_i \|\varepsilon(u)\|^2_{0,\Omega_i}$$
$$\geq \frac{\alpha_i}{C_i^2} \|\nabla u\|^2_{0,\Omega_i},$$

where $C_i > 0$ is the Korn constant in $H^1_{0,\Gamma_i}(\Omega_i)^d \subset H^1(\Omega_i)^d$, and $\alpha_i > 0$ is the ellipticity constant of $\mathbb{C}_i$.

For the interface terms, the coercivity assumption (A2) on M and S gives:

$$\int_\Sigma M \overline{u}|_\Sigma \cdot \overline{u}|_\Sigma \, ds \geq M_0 \|\overline{u}|_\Sigma\|^2_{0,\Sigma}, \quad \int_\Sigma S [\![u]\!]_\Sigma \cdot [\![u]\!]_\Sigma \, ds \geq S_0 \|[\![u]\!]_\Sigma\|^2_{0,\Sigma}.$$

Combining all contributions, we obtain:

$$a(u,u) \geq \frac{\alpha_1}{C_1^2} \|\nabla u\|^2_{0,\Omega_1} + \frac{\alpha_2}{C_2^2} \|\nabla u\|^2_{0,\Omega_2}$$
$$+ M_0 \|\overline{u}|_\Sigma\|^2_{0,\Sigma} + S_0 \|[\![u]\!]_\Sigma\|^2_{0,\Sigma}$$
$$\geq c_0 \|u\|^2_W,$$

where $c_0 := \min\left\{ \dfrac{\alpha_1}{C_1^2}, \dfrac{\alpha_2}{C_2^2} \right\} > 0.$

This establishes the coercivity of $a(\cdot,\cdot)$ on W.

Continuity of $a(\cdot,\cdot)$: To establish continuity of the bilinear form $a(u,w)$ on $W \times W$, we demonstrate the existence of a constant $c_1 > 0$ such that

$$|a(u,w)| \leq c_1 \|u\|_W \|w\|_W \quad \text{for all } u, w \in W.$$

The bilinear form consists of volume and interface terms. For the volume contributions, we use the boundedness of the elasticity tensors $\mathbb{C}_1$ and $\mathbb{C}_2$, together with inequality (2.7), to write:

$$\left| \int_{\Omega_i} \mathbb{C}_i \varepsilon(u) : \varepsilon(w)\, dx \right| \leq \|\mathbb{C}_i\|_{\infty,\Omega_i} \|\varepsilon(u)\|_{0,\Omega_i} \|\varepsilon(w)\|_{0,\Omega_i}$$
$$\leq \Lambda_i \|\nabla u\|_{0,\Omega_i} \|\nabla w\|_{0,\Omega_i},$$

for some constants $\Lambda_i > 0$ with $i = 1, 2$.

The interface terms are handled using the trace inequality. Since the functions $u \in W$ satisfy $u|_{\Omega_i} \in H^1_{0,\Gamma_i}(\Omega_i)^d$, and since $\Sigma \subset \partial\Omega_i$ is Lipschitz for $i = 1, 2$, the trace inequality, combined with the Poincaré inequality, implies that

$$\begin{aligned} \|\overline{u}|_\Sigma\|_{0,\Sigma} =& \frac{1}{2}\|u_1|_\Sigma + u_2|_\Sigma\|_{0,\Sigma} \le c_1\left(\|\nabla u_1\|_{0,\Omega_1} + \|\nabla u_2\|_{0,\Omega_2}\right) \le c_1'\|u\|_W, \\ \|[\![u]\!]_\Sigma\|_{0,\Sigma} =& \ \ \|u_2|_\Sigma - u_1|_\Sigma\|_{0,\Sigma} \le c_2\left(\|\nabla u_1\|_{0,\Omega_1} + \|\nabla u_2\|_{0,\Omega_2}\right) \le c_2'\|u\|_W. \end{aligned} \tag{2.8}$$

As a result, the interface terms in the bilinear form satisfy

$$\left|\int_\Sigma M\overline{u}|_\Sigma \cdot \overline{w}|_\Sigma \, ds\right| \le \|M\|_{\infty,\Sigma}\|\overline{u}|_\Sigma\|_{0,\Sigma}\|\overline{w}|_\Sigma\|_{0,\Sigma} \le C_M\|u\|_W\|w\|_W,$$

and

$$\left|\int_\Sigma S[\![u]\!]_\Sigma \cdot [\![w]\!]_\Sigma \, ds\right| \le \|S\|_{\infty,\Sigma}\|[\![u]\!]_\Sigma\|_{0,\Sigma}\|[\![w]\!]_\Sigma\|_{0,\Sigma} \le C_S\|u\|_W\|w\|_W.$$

Combining the volume and interface estimates, we conclude that all contributions of the bilinear form are bounded by a constant times $\|u\|_W\|w\|_W$, and thus $a(\cdot,\cdot)$ is continuous on $W \times W$.

Continuity of $\ell(\cdot)$: We now prove that the linear form

$$\ell(w) := \int_\Omega f \cdot w \, dx + \int_\Sigma h \cdot [\![w]\!]_\Sigma \, ds + \int_\Sigma g \cdot w|_\Sigma \, ds,$$

is continuous on W.

Using the Cauchy–Schwarz inequality and the trace regularity of functions in W, we estimate:

$$|\ell(w)| \le \|f\|_{0,\Omega}\|w\|_{0,\Omega} + \|h\|_{1/2,\Sigma}\|[\![w]\!]_\Sigma\|_{1/2,\Sigma} + \|g\|_{1/2,\Sigma}\|w|_\Sigma\|_{1/2,\Sigma}.$$

Therefore, by applying the Poincaré inequality to the volume term and using inequality (2.8) for the interface terms, there exists a constant $c_2 > 0$ such that:

$$|\ell(w)| \le c_2\left(\|f\|_{0,\Omega} + \|h\|_{1/2,\Sigma} + \|g\|_{1/2,\Sigma}\right)\|w\|_W,$$

which proves the continuity of ℓ on W.

The existence and uniqueness of the solution are guaranteed by the Lax–Milgram theorem.

A priori estimate. Let $u \in W$ be the unique solution to the variational problem:

$$a(u,w) = \ell(w) \quad \text{for all } w \in W.$$

By coercivity of the bilinear form $a(\cdot,\cdot)$ and continuity of $\ell(\cdot)$, there exists $c_0 > 0$, $c_2 > 0$ such that

$$c_0\|u\|_W^2 \le c_2\left(\|f\|_{0,\Omega} + \|h\|_{1/2,\Sigma} + \|g\|_{1/2,\Sigma}\right)\|u\|_W.$$

Assuming that $\|u\|_W \ne 0$, there exists a constant $C > 0$, independent of the data, such that

$$\|u\|_W \le C\left(\|f\|_{0,\Omega} + \|h\|_{1/2,\Sigma} + \|g\|_{1/2,\Sigma}\right).$$

$\square$

3. The elastic/elastic problem with interface jump conditions of Spring-Law type

We now consider the problem consisting of equations (2.1)–(2.3), along with interface jump conditions inspired by spring-law-type interface models:

$$[\![\sigma(u)\cdot n]\!]_\Sigma = Au|_\Sigma - g \quad \text{and} \quad [\![u]\!]_\Sigma = 0 \quad \text{on } \Sigma, \tag{3.1}$$

which gives the following problem denoted by (P_l):

$$\begin{cases} -\nabla\cdot\sigma_1(u) = f_1 \quad \text{in } \Omega_1, \\ -\nabla\cdot\sigma_2(u) = f_2 \quad \text{in } \Omega_2, \\ u = 0 \quad \text{on } \Gamma_1\cup\Gamma_2, \\ [\![\sigma(u)\cdot n]\!]_\Sigma = Au|_\Sigma - g \quad \text{on } \Sigma, \\ [\![u]\!]_\Sigma = 0 \quad \text{on } \Sigma, \end{cases} \tag{P_l}$$

where A satisfy the same assumption as M above, and $g\in H^{1/2}(\Sigma)^d$ is a given interface force.

Remark 3.1. In the case where $[\![u]\!]_\Sigma = q$ on Σ with $q\in H^{1/2}(\Sigma)^d$, we can apply a change of variable

$$\tilde{u}_1 := u_1 \quad \text{in } \Omega_1, \qquad \tilde{u}_2 := u_2 - v \quad \text{in } \Omega_2,$$

where $v\in H^1(\Omega_2)^d$ is the lifting (inverse of the trace mapping) of q.

Hence, it follows that

$$[\![\tilde{u}]\!]_\Sigma = 0 \quad \text{and} \quad [\![\sigma(\tilde{u})\cdot n]\!]_\Sigma = A\tilde{u}|_\Sigma - \tilde{g} \quad \text{on } \Sigma,$$

where $\tilde{g} := g + \sigma_2(v)\cdot n - (1/2)Aq$.

The proofs in the remainder of this paper are made for the zero-jump condition across the interface.

The corresponding weak formulation of problem (P_l) reads:

Find u in the subspace V of W, such that:

$$\begin{aligned} \int_{\Omega_1}\mathbb{C}_1\varepsilon(u):\varepsilon(w)\,dx + \int_{\Omega_2}\mathbb{C}_2\varepsilon(u):\varepsilon(w)\,dx + \int_\Sigma Au|_\Sigma\cdot w|_\Sigma\,ds \\ = \int_\Omega f\cdot w\,dx + \int_\Sigma g\cdot w\,ds, \quad \forall w\in V, \end{aligned} \tag{3.2}$$

where $V \equiv \{w\in W: \quad [\![w]\!]_\Sigma = 0 \quad \text{on } \Sigma\}$.

Corollary 3.2 (Well-posedness for S-L.I.C. model)**.** *Let $f_i\in L^2(\Omega_i)^d$ for $i=1,2$, and let $g\in H^{1/2}(\Sigma)^d$. If $\mathbb{C}_1$ and $\mathbb{C}_2$ satisfy assumption (A1), and A satisfies assumption (A2), then there exists a unique solution $u\in V$ to the weak form (3.2).*

Furthermore, for some constant $C>0$ the following estimate holds:

$$\|u\|_W \le C\left(\|f\|_{0,\Omega} + \|g\|_{1/2,\Sigma}\right).$$

The proof of this corollary will not be presented here, as it is straightforward and follows directly from the Lax-Milgram theorem.

4. Penalized problem of elastic–elastic model with J.E.B.C.

Let us consider the penalized problem, denoted by (P_r), given by (2.1)-(2.5) with $h = 0$, $M = A$ and $S = \frac{1}{r}\boldsymbol{I}$. The weak form of the penalized problem (P_r) reads, for all $r > 0$:

Find $u_r \in W$ such that:

$$\begin{aligned}\int_{\Omega_1} \mathbb{C}_1\varepsilon(u_r) : \varepsilon(w)\, dx + \int_{\Omega_2} \mathbb{C}_2\varepsilon(u_r) : \varepsilon(w)\, dx + \int_\Sigma M\overline{u}_r|_\Sigma \cdot \overline{w}|_\Sigma\, ds \\ + \frac{1}{r}\int_\Sigma [\![u_r]\!]_\Sigma \cdot [\![w]\!]_\Sigma\, ds = \int_\Omega f\cdot w\, dx + \int_\Sigma g\cdot w\, ds, \quad \forall w \in W.\end{aligned} \tag{4.1}$$

Equivalently, the solution of (3.2) arises as the limit of the penalized problem (4.1) as the penalty parameter r tends to zero. The theorem below makes this convergence precise.

Theorem 4.1 (Convergence to the elastic/elastic model with S-L.I.C.). *Let $f_i \in L^2(\Omega_i)^d$ for $i = 1, 2$, let $g \in H^{1/2}(\Sigma)^d$, and for each $r > 0$, let $u_r \in W$ be the unique weak solution of the penalized problem (P_r) (i.e., the solution of (4.1)).*

Then, as $r \to 0$, the sequence (u_r) converges strongly in W to the unique solution u of the weak form (3.2), with $[\![u]\!]_\Sigma = 0$ satisfied automatically.

Moreover, there exist two constants $C > 0$ and $C'(f_1, f_2, g) > 0$, independent of r, such that:

$$\|u_r - u\|_W \le C\sqrt{r}, \quad \text{and} \quad \|[\![u_r]\!]_\Sigma\|_{0,\Sigma} \le C' r.$$

Proof. We aim to show that the family $(u_r)_{r>0} \subset W$, consisting of solutions to the penalized problem (P_r), converges strongly in W to the unique solution $u \in V$ of the limit problem, with $[\![u]\!]_\Sigma = 0$. Before starting, let us assume that $\|u_r\|_W \neq 0$ and $\|[\![u_r - u]\!]_\Sigma\|_{0,\Sigma} \neq 0$; the cases where these quantities vanish are trivial and require no special handling.

Uniform estimate: Choosing $w = u_r$ in the weak form (4.1) and applying Korn's inequality and the coercivity of $\mathbb{C}_1$ and $\mathbb{C}_2$, we get for $i = 1, 2$

$$\int_{\Omega_i} \mathbb{C}_i\varepsilon(u) : \varepsilon(u)\, dx \ge \alpha_i \int_{\Omega_i} |\varepsilon(u)|^2\, dx \ge \frac{\alpha_i}{C_i}\int_{\Omega_i} |\nabla u|^2\, dx,$$

where $\alpha_i > 0$ and $C_i > 0$ are the coercivity constant of $\mathbb{C}_i$ and Korn's constant respectively, for $i = 1, 2$. That yields

$$\begin{aligned} c_0' \int_{\Omega_1\cup\Omega_2} |\nabla u|^2\, dx + \int_\Sigma M\overline{u}_r|_\Sigma \cdot \overline{u}_r|_\Sigma\, ds + \frac{1}{r}\int_\Sigma [\![u_r]\!]_\Sigma \cdot [\![u_r]\!]_\Sigma\, ds \\ \le C\left(\|f\|_{0,\Omega} + \|g\|_{1/2,\Sigma}\right)\|u_r\|_W,\end{aligned} \tag{4.2}$$

where $c_0' = \min\{\frac{\alpha_1}{C_1}, \frac{\alpha_2}{C_2}\}$ and $C > 0$.

Using the coercivity of $a(\cdot,\cdot)$, we obtain:

$$c\|u_r\|_W^2 + \frac{1}{r}\|[\![u_r]\!]_\Sigma\|_{0,\Sigma}^2 \le C\left(\|f\|_{0,\Omega} + \|g\|_{1/2,\Sigma}\right)\|u_r\|_W. \tag{4.3}$$

Dropping the interface term in the left-hand side and divide both sides by $c\|u_r\|_W$ to obtain, for a constant $c' > 0$:

$$\|u_r\|_W \leq c' \left(\|f\|_{0,\Omega} + \|g\|_{1/2,\Sigma}\right). \tag{4.4}$$

Again dropping a term in the left-hand side of (4.3), but this time we drop $c\|u_r\|_W$, then by using inequality (4.4) to the bound $\|u_r\|_W$ in the right-hand side of (4.3) we obtain:

$$\|[\![u_r]\!]_\Sigma\|_{0,\Sigma} \leq C'\sqrt{r}. \tag{4.5}$$

where $C' = C'(f_1, f_2, g) > 0$ is a constant depending of the data.

Convergence as $r \to 0$: From the uniform bound (4.4), the family $(u_r)_{r>0} \subset W$ is bounded in the Hilbert space W. Therefore, by the Banach–Alaoglu theorem, there exists a function $u \in W$ and a subsequence (still denoted u_r) such that

$$u_r \rightharpoonup u \quad \text{weakly in } W \quad \text{as } r \to 0.$$

Moreover, by the compact embedding $W \hookrightarrow L^2(\Omega)^d$, this convergence is strong in $L^2(\Omega)^d$.

In addition, from the uniform bound (4.5), the rescaled family $\left(\dfrac{1}{\sqrt{r}}[\![u_r]\!]_\Sigma\right)_{r>0}$ is bounded in the Hilbert space $L^2(\Sigma)^d$. Thus, by the Banach–Alaoglu theorem, there exists a function $\psi \in L^2(\Sigma)^d$ and a subsequence (still indexed by r) such that

$$\frac{1}{\sqrt{r}}[\![u_r]\!]_\Sigma \rightharpoonup \psi \quad \text{weakly in } L^2(\Sigma)^d \quad \text{as } r \to 0.$$

Moreover, we have $[\![u_r]\!]_\Sigma \to 0$ as $r \to 0$. Since the trace operator is continuous from W to $L^2(\Sigma)^d$, and $[\![u_r]\!]_\Sigma$ converges strongly to zero in $L^2(\Sigma)^d$, it follows that

$$[\![u]\!]_\Sigma = 0.$$

Therefore, u belongs to $V \subset W$.

Taking the limit $r \to 0$ in the weak formulation (4.1) with $w \in V$ and noting that $\overline{u}|_\Sigma = u|_\Sigma$, we recover the limit problem:

$$\int_{\Omega_1} \mathbb{C}_1\varepsilon(u) : \varepsilon(w)\,dx + \int_{\Omega_2} \mathbb{C}_2\varepsilon(u) : \varepsilon(w)\,dx + \int_\Sigma Mu\cdot w\,ds = \int_\Omega f\cdot w\,dx + \int_\Sigma g\cdot w\,ds,$$

which admits a unique solution in V as stated in corollary 3.2.

Error estimate: Let u_r and u be the solutions satisfying their respective variational formulations, we subtract them to obtain:

$$\int_{\Omega_1} \mathbb{C}_1|\varepsilon(u_r - u)|^2\,dx + \int_{\Omega_2} \mathbb{C}_2|\varepsilon(u_r - u)|^2\,dx + \int_\Sigma M|\overline{u}_{r|\Sigma} - u|^2\,ds$$
$$+\frac{1}{r}\|[\![u_r - u]\!]_\Sigma\|_{0,\Sigma}^2 = \int_\Sigma \psi\cdot[\![u_r - u]\!]_\Sigma\,ds.$$

Using the coercivity of $\mathbb{C}_1, \mathbb{C}_2$ and M and Cauchy-Scwharz inequality, we get

$$\begin{aligned}&\alpha_0\int_{\Omega_1\cup\Omega_2} |\varepsilon(u_r - u)|^2\,dx + M_0\|\overline{u}_{r|\Sigma} - u\|_\Sigma^2\\ &+\frac{1}{r}\|[\![u_r - u]\!]_\Sigma\|_{0,\Sigma}^2 \leq \|\psi\|_{0,\Sigma}\|[\![u_r - u]\!]_\Sigma\|_{0,\Sigma},\end{aligned} \tag{4.6}$$

where $\alpha_0 = \min\{\alpha_1, \alpha_2\}$.

Dropping some positive terms in the left-hand side and multiplying by $r/\|[\![u_r - u]\!]_\Sigma\|_{0,\Sigma}$ we get:

$$\|[\![u_r - u]\!]_\Sigma\|_{0,\Sigma} \leq r\|\psi\|_{0,\Sigma}. \tag{4.7}$$

Since $[\![u]\!]_\Sigma = 0$, we have

$$\|[\![u_r - u]\!]_\Sigma\|_{0,\Sigma} = \|[\![u_r]\!]_\Sigma - [\![u]\!]_\Sigma\|_{0,\Sigma} = \|[\![u_r]\!]_\Sigma\|_{0,\Sigma},$$

and thus the error estimate becomes

$$\|[\![u_r]\!]_\Sigma\|_{0,\Sigma} \leq r\|\psi\|_{0,\Sigma}.$$

Applying Young's inequality $ab \leq a^2/2r + b^2r/2$ to the right-hand side of (4.6), we obtain

$$\begin{aligned}\alpha_0\|\varepsilon(u_r - u)\|^2_{0,\Omega} + M_0\|\overline{u}_{r|\Sigma} - u\|^2_{0,\Sigma} + \frac{1}{r}\|[\![u_r - u]\!]_\Sigma\|^2_{0,\Sigma}\\ \leq \frac{1}{2r}\|[\![u_r - u]\!]_\Sigma\|^2_{0,\Sigma} + \frac{r}{2}\|\psi\|^2_{0,\Sigma}.\end{aligned}$$

Now subtract $\frac{1}{2r}\|[\![u_r - u]\!]\|^2_{0,\Sigma}$ from both sides:

$$\alpha_0\|\varepsilon(u_r - u)\|^2_{0,\Omega} + M_0\|\overline{u_r} - u\|^2_{0,\Sigma} + \frac{1}{2r}\|[\![u_r - u]\!]\|^2_{0,\Sigma} \leq \frac{r}{2}\|\psi\|^2_{0,\Sigma}.$$

Applying Korn's inequality to the first term and dropping the other terms on the left-hand side, we obtain

$$\frac{\alpha_0}{C_0}\|(u_r - u)\|^2_W \leq \frac{r}{2}\|\psi\|^2_{0,\Sigma},$$

where $C_0 = \max\{C_1, C_2\} > 0$ with C_1 and C_2 are Korn's constants in Ω_1 and Ω_2 respectively. That leads to the final estimate

$$\|u_r - u\|_W \leq C\sqrt{r},$$

where $C(\psi) > 0$.

Thus, the proof is complete. □

5. Finite Volume discretization

We introduce a finite volume-based treatment of the linear elastic/elastic problem with J.E.B.C. over the domain $\Omega = \Omega_1 \cup \Sigma \cup \Omega_2$. Each subdomain is divided into a uniform Cartesian grid of non-overlapping rectangular control volumes K, with cell center denoted by x_K, and neighboring cells L with center x_L, enabling second-order accurate approximations using simple stencil-based schemes. This approach is widely applied in previous research in fluid dynamics [5, 4, 3] or in elasticity [6].

5.1. **Admissible meshes.** Let $\Omega = \Omega_1 \cup \Sigma \cup \Omega_2 \subset \mathbb{R}^d$ be a bounded open set (square for $d = 2$ or cube for $d = 3$). Let $\mathcal{D} = (\mathcal{M}, \mathcal{E}, \mathcal{P})$ denotes an admissible mesh (with $\mathcal{M} = \mathcal{M}_1 \cup \mathcal{M}_2$) as defined in [5], that is, for $i = 1, 2$:

Ω_i is partitioned into a finite sequance of convex subsets $\mathcal{M}_i$ of $\mathbb{R}^d$ (squares for $d = 2$ or cubes for $d = 3$). The elements $K \in \mathcal{M}_i$ are called control volumes of nonzero measure m_K.

Each control volume $K \in \mathcal{M}_i$ has the set $\mathcal{E}_K$ of edges (segments for $d = 2$ and squares for $d = 3$) e of size m_e and each edge e_K of K has a unit normal vector $\mathbf{n}_{e,K}$ outward to K. All edges in the mesh are collected in the set $\mathcal{E} = \bigcup_{K \in \mathcal{M}_1 \cup \mathcal{M}_2} \mathcal{E}_K = \mathcal{E}_{int} \cup \mathcal{E}_{ext} \cup \mathcal{E}_\Sigma$, where $\mathcal{E}_{int}$ include the interior edges (edges that does not coincide with Γ_1, Γ_2 and Σ), $\mathcal{E}_{ext}$ contains the exterior edges (edges that coincide with Γ_1 or Γ_2), and $\mathcal{E}_\Sigma$ is consists of the edges of which overlap with Σ.

We refer with $\mathcal{P}$ to the set of points $(\mathbf{x}_K)_{K \in \mathcal{M}_i}$ satisfying the orthogonality condition.

The Euclidean distance $d(\mathbf{x}_K, e_K)$ is denoted $d_{K,e}$. For any $K \in \mathcal{M}_i$ and $L \in \mathcal{N}_K$ ($\mathcal{N}_K$ the neighboring control volumes of K), we denote by $e_{K|L} \in \mathcal{E}_K \cup \mathcal{E}_L$ the common edge between K and L we then abbreviate $\mathbf{n}_{KL} := \mathbf{n}_{K,K|L}$, we also set $d_{KL} = d_{K,K|L} + d_{L,K|L}$ the Euclidean distance $d(\mathbf{x}_K, \mathbf{x}_L)$.

5.2. **Treatement of Internal cells.** In our model, the stress tensor is given by the classical isotropic elasticity law $\sigma(u) = \lambda\,(\nabla \cdot u)\,\boldsymbol{I} + 2\mu\varepsilon(u)$, with $\varepsilon = \frac{1}{2}\left(\nabla u + (\nabla u)^\top\right)$. For a face $e \in \mathcal{E}_{int}$ shared by cells K and L both in $\mathcal{M}_1$ (or both in $\mathcal{M}_2$), with unit normal $n_{e,K}$ from K to L, we approximate the gradient of u in the direction of $n_{e,K}$ by

$$\nabla u|_e \approx \frac{u_L - u_K}{d_{KL}} \otimes n_{e,K},$$

where $\otimes$ denotes the tensor (or dyadic) product, d_{KL} is the distance between the centers of K and L, and we denote by u_K and u_L the cell-centered finite volume approximations of the displacement field u in the cells K and L, respectively. This gives a directional approximation of the displacement gradient.

From this, the symmetric strain tensor is approximated by

$$\varepsilon(u)|_e \approx \frac{1}{2d_{KL}}\left[(u_L - u_K) \otimes n_{e,K} + n_{e,K} \otimes (u_L - u_K)\right],$$

and the divergence of u is approximated by

$$(\nabla \cdot u)|_e \approx \frac{(u_L - u_K) \cdot n_{e,K}}{d_{KL}}.$$

Substituting into the stress tensor, we obtain the following discrete approximation of the normal stress on face e with respect to cell K:

$$\sigma_K \cdot n_{e,K} \approx \left(\lambda \frac{(u_L - u_K) \cdot n_{e,K}}{d_{KL}}\right) n_{e,K} + \frac{\mu}{d_{KL}}\left[(u_L - u_K) + ((u_L - u_K) \cdot n_{e,K})\, n_{e,K}\right].$$

An analogous formula holds for $\sigma_L \cdot n_{e,K}$ (i.e., stress evaluated from cell L, but still projected in the direction of $n_{e,K}$).

At the outer boundary of the domain, Dirichlet conditions are enforced by prescribing the value of the unknown u_K at boundary control volumes adjacent to the Dirichlet boundary. However, at the interface Σ, where jump and average transmission conditions are imposed, we do not use the above flux expressions directly. Instead, we derive the interface fluxes by enforcing the transmission conditions (2.4)–(2.5), and combine them with the cell-centered unknowns u_K and u_L, as shown is the next subsection.

5.3. **Treatment of the Interface Conditions on Σ.** Let $e \in \mathcal{E}_\Sigma$ be the common face between the control volumes $K \in \mathcal{M}_1$ and $L \in \mathcal{M}_2$. We denote by $n_{e,K}$ the unit normal on e that points outward from K and by $n_{e,L} = -n_{e,K}$ the outward normal from L. Define the normal stresses with respect to the same geometric normal $n_{e,K}$ by

$$\tau_K := \sigma_K\, n_{e,K}, \qquad \tau_L := \sigma_L\, n_{e,K},$$

where $\sigma_K := \sigma_1(u_K)$ and $\sigma_L := \sigma_2(u_L)$.

The continuous interface conditions read

$$\llbracket \sigma(u)\cdot n \rrbracket_\Sigma = M\, \overline{u}\big|_\Sigma - g,$$
$$\overline{\sigma(u)\cdot n}\big|_\Sigma = S\, \llbracket u \rrbracket_\Sigma - h.$$

Because the finite-volume method stores unknowns at cell centres, the natural first-order approximations on e are

$$\llbracket u \rrbracket_\Sigma \approx u_L - u_K, \qquad \overline{u}\big|_\Sigma \approx \frac{u_K + u_L}{2}.$$

Using the same normal $n_{e,K}$ for both sides, the jump and average of the normal stress become

$$\llbracket \sigma(u)\cdot n \rrbracket_\Sigma = \tau_L - \tau_K, \qquad \overline{\sigma(u)\cdot n}\big|_\Sigma = \frac{\tau_L + \tau_K}{2}.$$

Substituting these discrete counterparts of the jump and average into (2.4)–(2.5) yields the linear system

$$\begin{cases} \tau_L - \tau_K = \dfrac{M}{2}\,(u_K + u_L) - g, \\[2mm] \dfrac{\tau_L + \tau_K}{2} = S\,(u_L - u_K) - h. \end{cases} \tag{5.1}$$

Solving (5.1) for τ_K and τ_L, and recalling the definitions of τ_K and τ_L and the fact that both are expressed with respect to the single normal $n_{e,K}$, we arrive at the discrete interface flux condition

$$\begin{cases} \sigma_K \cdot n_{e,K} = (S - \dfrac{1}{4}M)u_L - (S + \dfrac{1}{4}M)u_K - g + \dfrac{1}{2}h, \\[2mm] \sigma_L \cdot n_{e,K} = (S + \dfrac{1}{4}M)u_L - (S - \dfrac{1}{4}M)u_K - g - \dfrac{1}{2}h. \end{cases} \tag{5.2}$$

Widely encountered cases in the literature related to classical elastic-elastic interaction problems can be derived from these conditions, and are special cases of the more comprehensive framework presented. By appropriately choosing the parameters in the interface conditions, we recover several well-known scenarios,

Case N°	Interface conditions	Parameters on Σ
1	no-slip and stress continuity conditions	$h = g = 0, M = 0, S = \frac{1}{r}I$
2	slip and stress continuity conditions	$h = 0, g = \frac{1}{r}q, M = rI, S = \frac{1}{r}I$
3	no-slip and stress discontinuity conditions	$h \neq 0, g = 0, M = rI, S = \frac{1}{r}I$
4	slip and stress discontinuity conditions	$h \neq 0, g = \frac{1}{r}q, M = rI, S = \frac{1}{r}I$
5	Separate Fourier conditions	$S = \frac{1}{4}M = \frac{1}{r}I$

Table 1. Interface condition cases

which provide important insights and applications in various physical contexts. For that, let $r > 0$ be a real penalty parameter and let I be the identity matrix, different cases based on the choix of S, M, g and h are summerized in table 1.

5.4. **Linear algebraic system.** The final algebraic system is assembled for each displacement component resulting in:

$$\begin{pmatrix} A_1 & B \\ B & A_2 \end{pmatrix} \begin{pmatrix} U_x \\ U_y \end{pmatrix} = \begin{pmatrix} F_x \\ F_y \end{pmatrix} \tag{5.3}$$

where U_x and U_y are the descrete unknowns, and F_x, F_y are the descretization of source term using the mid-point rule, consistent with the FVM framework (we note that both vectors U_x and U_y both contain unknowns from Ω_1 and Ω_2 classified in a specific order based on our programming, and the vectors F_x and F_y also contain both source terms f_1 and f_2 and some lines also contain the interface contributions g and h). The linear system is solved iteratively using Preconditioned Conjugate Gradient, GMRES or Incomplete Cholesky preconditioned solvers.

6. Numerical Tests

In this section, we present numerical experiments to validate the accuracy and efficiency of the proposed model. The tests are performed on both homogeneous and heterogeneous isotropic media, with comparisons to analytical solutions where available. The discrete relative error in the $\mathbb{L}^2$-norm and the associate convergence rate are computed as:

$$E_h = \frac{\|U_{ex} - U_h\|_{\mathbb{L}^2(\Omega_h)}}{\|U_{ex}\|_{\mathbb{L}^2(\Omega_h)}}, \qquad \text{and} \qquad cv.rate = \frac{log\left(E_{h_{k+1}}\right) - log\left(E_{h_k}\right)}{log\left(h_{k+1}\right) - log\left(h_k\right)} \tag{6.1}$$

where U_{ex} is the vector of exact solution of the limit problem computed in the centers of CVs, and U_h is the vector of numerical solution.

In what follows, u_i is originally composed of two components $u_i = \left(u_i^{(1)}, u_i^{(2)}\right)^\top$, but for simplicity we suppose the components are equals (i.e. $u_i^{(1)} = u_i^{(2)}$ for $i = 1, 2$). We choose Young's modulus $E \approx 1.5429 \times 10^5 MPa$ and Poisson's ratio $\nu \approx 0.2857$, the Lame's coefficients corresponding to this values are $\lambda =$

$8 \times 10^5 MPa$ and $\mu = 6 \times 10^5 MPa$ for some engineering materials (e.g., titanium alloys, stiff steels or high-performance ceramics). To better understand the geometric configurations addressed in the following test cases, we illustrate in Figure 1 three typical interface layouts between two subdomains.

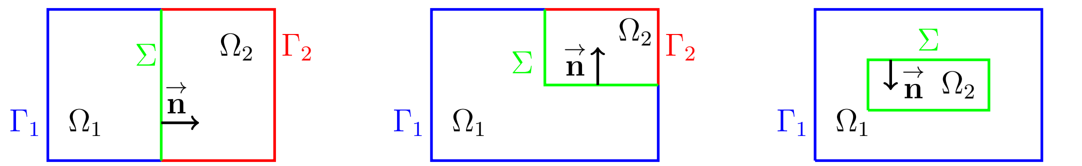

(A) Vertical Interface (B) L-shaped Interface (C) Rectangular Interface

FIGURE 1. Illustration of different interface configurations between two subdomains.

6.1. **From Penalized Interface to Continuity Condition.** In the first set of numerical experiments, we investigate the convergence of the proposed penalized interface formulation toward the classical *continuity condition*. This test is designed to validate the effectiveness of the penalization approach in approximating strong coupling conditions as the penalization parameter tends to zero. To this end, we consider two distinct interface geometries: the *L-shaped interface*, where the interface exhibits a corner structure connecting horizontal and vertical segments, and the *rectangular embedded interface*, where the interface surrounds a fully enclosed subdomain. These two configurations, illustrated in Figure 1, represent challenging geometries for interface problems and allow us to assess the method's accuracy in both standard and complex interface topologies. The convergence behavior is quantified by computing the difference between the solutions obtained with the penalized interface and those satisfying the exact continuity condition.

Test Case 1: L-Shaped Interface. We first validate the finite volume scheme on a unit square domain $\Omega = [0, 1.5]^2$ which is devided in two non-overlapping subregions $\Omega_1 = \Omega_x \cup \Omega_y$ and $\Omega_2 = [1, 1.5]^2$, with $\Omega_x = \{(x, y) \in \Omega \mid 0 < x < 1 \text{ and } 0 < y < 1.5\}$ and $\Omega_y = \{(x, y) \in \Omega \mid 0 < y < 1 \text{ and } 0 < x < 1.5\}$. Ω is meshed with uniform square cells of grid steps h ranging from $1/9$ to $1/60$. We consider the following interaction problem

$$\begin{cases} -\nabla \cdot \sigma_1(u) = f_1 & \text{in } \Omega_1, \\ -\nabla \cdot \sigma_2(u) = f_2 & \text{in } \Omega_2, \\ u = 0 & \text{on } \Gamma_1 \cup \Gamma_2, \\ [\![\sigma(u) \cdot n]\!]_\Sigma = g & \text{on } \Sigma \\ \overline{\sigma(u) \cdot n}|_\Sigma = \dfrac{1}{2r}[\![u]\!]_\Sigma & \text{on } \Sigma. \end{cases} \tag{P_L}$$

where $\sigma_1(u) = \sigma_2(u) = \lambda(\nabla \cdot u)\boldsymbol{I} + 2\mu\varepsilon(u)$. As stated in theorem 4.1, the solution of (P_L) tends to the solution of problem (P_l) with continuity condition ($[\![u]\!]_\Sigma = 0$).

The analytical solution of the problem (P_l) is

$$u_1(x,y) = 10xy(x-1)(y-1)(x-1.5)(y-1.5),$$
$$u_2(x,y) = 10(x-1)(y-1)(x-1.5)(y-1.5),$$

where u_i is the exact solution in Ω_i for $i = 1, 2$. The source terms f_1 and f_2 are constructed to satisfy the equations in Problem (P_L), and g is defined by

$$g(x,y) = \begin{cases} \begin{pmatrix} 5(2\mu+\lambda)(y-1)^2\left(y-\frac{3}{2}\right) \\ 5\mu(y-1)^2\left(y-\frac{3}{2}\right) \end{pmatrix}, & \text{if } x = 1,\ 1 \le y \le 1.5, \\ \begin{pmatrix} 5\mu x(x-1)\left(x-\frac{3}{2}\right) \\ 5\lambda(x-1)^2\left(x-\frac{3}{2}\right) \end{pmatrix}, & \text{if } y = 1,\ 1 \le x \le 1.5. \end{cases}$$

The problem (P_L) is solved with different step-sizes h and a penalty parameter $r = h/(2\mu+\lambda)$. Table 2 summarizes the relative $\mathbb{L}^2$-norm errors for varying grid steps h.

TABLE 2. Relative errors for solutions of test case 1.

h	$1/9$	$1/18$	$1/30$	$1/60$
$\frac{\lVert U_{ex}-U_h\rVert}{\lVert U_{ex}\rVert}$	5.5850×10^{-2}	1.8189×10^{-2}	9.9357×10^{-3}	4.8002×10^{-3}

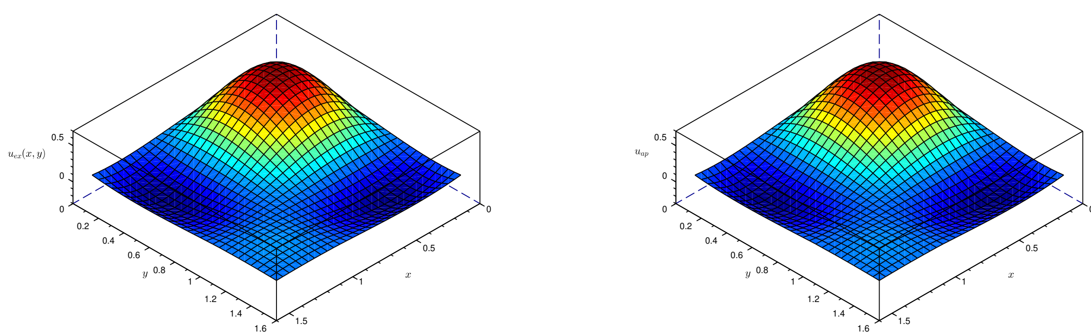

(A) Analytical solution (B) Numerical solution

FIGURE 2. Analytical and numerical solutions of test case 1.

In addition to the results presented in Table 2, Figure 2 shows a comparison between the analytical solution of Problem (P_l) and the numerical solution of Problem (P_L). As can be seen, the two solutions are almost identical, demonstrating the high accuracy and robustness of the discretization method, as well as the effective convergence of the numerical solution of Problem (P_L) toward the analytical solution of the no-slip interaction problem (P_l). In Figure 3, the subfigure (a) depicts the projection of both analytical and numerical solutions on $y = x$, while subfigure (b) demonstrates a convergence rate between 1 and 2 (i.e. $1 \le cv.\ rate \le 2$) of the penalized problem (P_L), which validate the results in Table 2 and Figure 2.

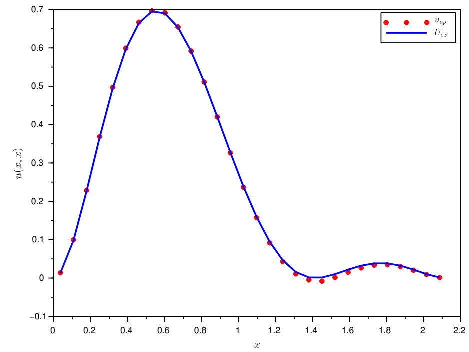

(A) Projection of solutions in the segment $y = x$

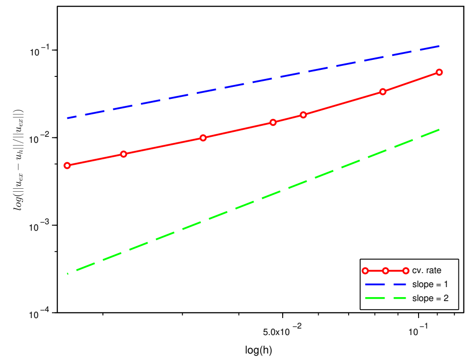

(B) Convergence rate

FIGURE 3. Projection of solutions on $y = x$ and convergence rate of test case 1.

<u>*Test Case 2: Rectangular Interface.*</u> For this case the interface Σ will take an rectangular shape. For that, let $\Omega = [0, 1]^2$ be a rectangular domain subdevided in $\Omega_2 = [1/3, 2/3]^2$ and $\Omega_1 = \Omega \backslash \Omega_2$.

We reconsider the problem (P_L) is the new domain configuration, which will be denoted by (P_R). The analytical solution of the corresponding limit problem (P_l) is chosen as

$$u_1(x, y) = 10xy(x-1)(y-1)\left(x-\frac{1}{3}\right)\left(y-\frac{1}{3}\right)\left(x-\frac{2}{3}\right)\left(y-\frac{2}{3}\right),$$
$$u_2(x, y) = \left(x-\frac{1}{3}\right)\left(y-\frac{1}{3}\right)\left(x-\frac{2}{3}\right)\left(y-\frac{2}{3}\right),$$

where u_i is the exact solution in Ω_i for $i = 1, 2$. The source terms f_1, f_2 and the stress jump g are constructed to satisfy the equations in Problem (P_R), The problem (P_R) is solved with different step-sizes h and a penalty parameter $r = h^2/(2\mu+\lambda)$. Table 3 summarizes the relative $\mathbb{L}^2$-norm errors for diverse grid steps h and r dependent of h.

TABLE 3. Relative errors for solutions of test case 2.

h	$1/9$	$1/18$	$1/30$	$1/60$
$\frac{\|U_{ex}-U_h\|}{\|U_{ex}\|}$	5.5850×10^{-2}	1.8188×10^{-2}	9.9356×10^{-3}	4.8002×10^{-3}

In Figure 4, the subfigure (a) illustrate the projection of both analytical and numerical solution on the segment $y = x$ for $h = 1/45$, which shows a good accuracy and robustness, while subfigure (b) demonstrates a convergence rate close to 1 of the penalized problem (P_R) for different step sizes $1/9 \leq h \leq 1/45$ and for a fixed $r = \min(h)^2/(2\mu + \lambda)$, which validate the results in Table 3.

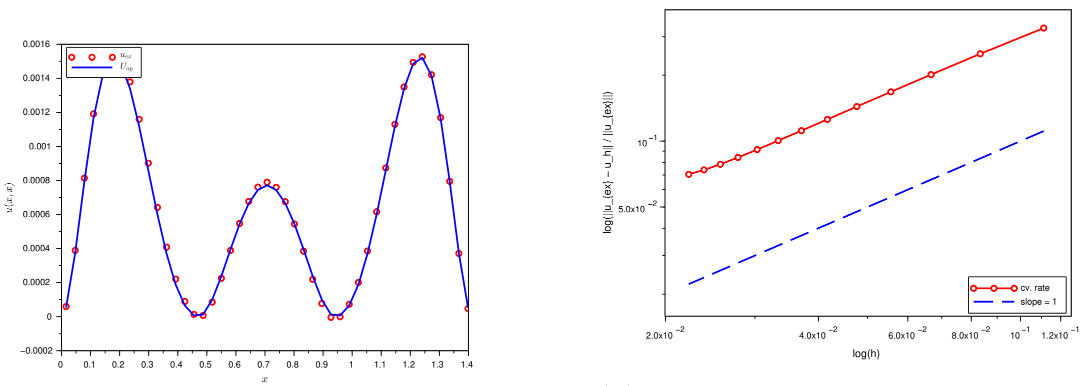

(A) Projection of solutions on $y = x$.

(B) Convergence rate for $r = \min(h)^2/(2\mu + \lambda)$.

FIGURE 4. Projection of solutions on $y = x$ and convergence rate of test case 2.

6.2. **From Penalized Interface to Discontinuity Condition.** In the second set of numerical experiments, we examine the convergence of the penalized interface formulation toward the classical *discontinuity interface condition* ($[\![u]\!]_\Sigma \neq 0$). To evaluate this behavior, we consider a simplified geometry involving a *vertical interface* between two subdomains. This configuration, shown in Figure 1, facilitates the assessment of the method's ability to recover the expected discontinuous behavior. This test shows the numerical penalized solution approximates the exact solution satisfying the discontinuity condition as the penalization parameter tends to zero.

Test Case 3: Vertical Interface. Let $\Omega = [0, 1.5] \times [0, 1]$ be a rectangular domain subdevided in $\Omega_1 = [0, 1] \times [0, 1]$ and $\Omega_2 = [1, 1.5] \times [0, 1]$, and let the interface $\Sigma = \{x = 1\} \times [0, 1]$.

The same previous problem, now denoted by (P_V), is reconsidered in the new configuration. The analytical solution of the respective limit problem (P_l) with $[\![u]\!]_\Sigma = \frac{1}{2}\sin(\pi y) - y(y-1)$ is given by

$$\begin{aligned} u_1(x, y) &= x\left(x - \frac{3}{2}\right)\sin(\pi y), \\ u_2(x, y) &= y(y-1)\cos(\pi x). \end{aligned}$$

The source terms f_1 and f_2 are constructed to satisfy the equations in problem (P_V), and the stress jump g is defined, for every $y \in [0, 1]$, by

$$g(y) = \begin{pmatrix} \frac{2\mu+\lambda}{2}\sin(\pi y) + \lambda\left[-\frac{\pi}{2}\cos(\pi y) + (2y-1)\right] \\ \mu\left[-\frac{\pi}{2}\cos(\pi y) + (2y-1) + \frac{1}{2}\sin(\pi y)\right] \end{pmatrix}.$$

In Figure 5, We examine how the convergence rate varies as the penalization parameter is decreased, setting $r = \min(h)/(K(2\mu + \lambda))$ for different grid step sizes h ranging from $1.5/9$ to $1.5/60$ and for K values in $\{1, 10, 25, 50, 100\}$. The results in the figure indicate that the convergence rate generally lies between slopes of 1 and 2 for $K = \{5, 10, 50\}$, while for $K = 100$ and the finest mesh $h = 1.5/60$, the performance deteriorates, yielding lower convergence rates.

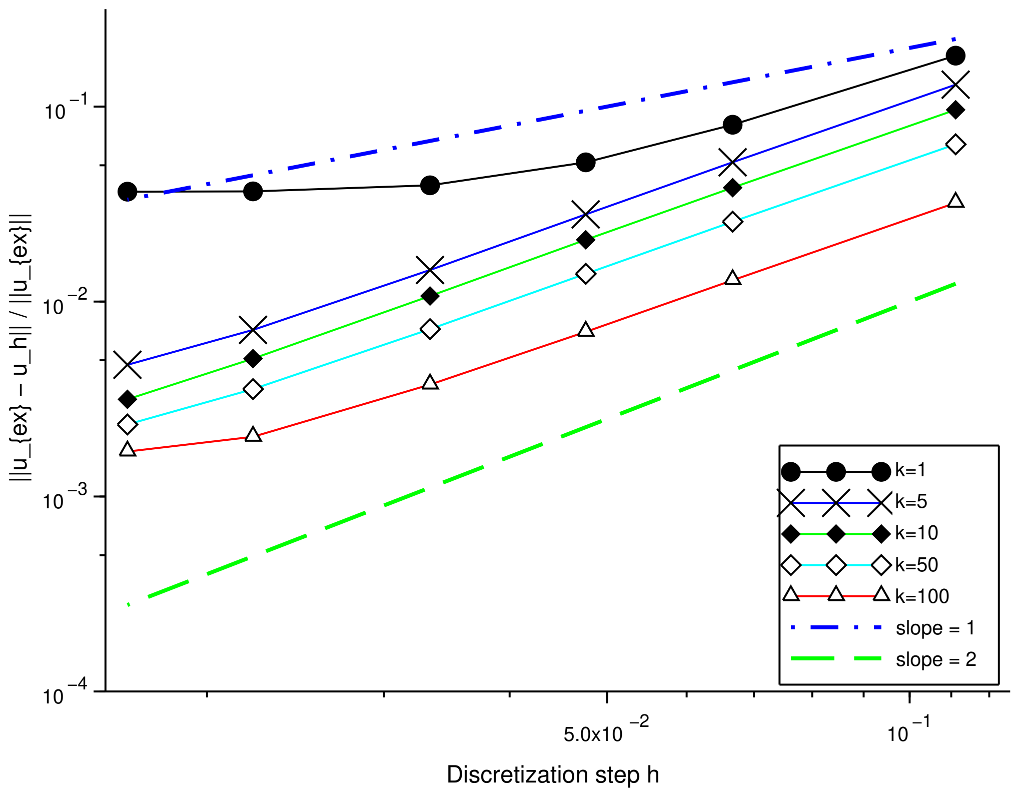

FIGURE 5. Effect of penalization to the cv.rate in test case 3.

7. Conclusions

This work has rigorously established the well-posedness of elastic–elastic interaction problems governed by jump-embedded boundary conditions (J.E.B.C.), providing a unified mathematical framework for coupled systems with discontinuous interface responses. By leveraging tools from functional analysis, we demonstrated the strong convergence of the J.E.B.C. model toward spring-type transmission conditions and derived a priori error estimates for its penalized approximation.

Numerical experiments across diverse configurations (vertical, L-shaped, and rectangular interfaces) confirmed the method's robustness, accuracy, and convergence under grid refinement.

To the best of our knowledge, this study is the first to bridge the gap between theoretical analysis and computational methodology for purely elastic J.E.B.C. systems, generalizing earlier fictitious domain approaches beyond fluid–porous interactions. Future work should focus on extending this framework to more complex multiphysics scenarios, such as interaction models with moving boundaries and interface, ot fluid-elastic interactions (FSI).

References

[1] Angot, P. (2010). A fictitious domain model for the Stokes/Brinkman problem with jump embedded boundary conditions. Comptes Rendus Mathematique, 348(11-12), 697-702. https://doi.org/10.1016/j.crma.2010.04.022

[2] Angot, P. (2011). On the well-posed coupling between free fluid and porous viscous flows. Applied mathematics letters, 24(6), 803-810. https://doi.org/10.1016/j.aml.2010.07.008

[3] Boukabache, A., and Kechkar, N. (2019). A unified stabilized finite volume method for Stokes and Darcy equations. Journal of the Korean Mathematical Society, 56(4), 1083-1112. https://doi.org/10.4134/JKMS.j180641

[4] Chénier, E., Eymard, R., Herbin, R., and Touazi, O. (2008). Collocated finite volume schemes for the simulation of natural convective flows on unstructured meshes. International journal for numerical methods in fluids, 56(11), 2045-2068. https://doi.org/10.1002/fld.1603

[5] Ciarlet, P. G., and Lions, J. L. (Eds.). (1990). *Handbook of numerical analysis* (Vol. 11). Gulf Professional Publishing.

[6] Jasak, H., and Weller, H. G. (2000). Application of the finite volume method and unstructured meshes to linear elasticity. International journal for numerical methods in engineering, 48(2), 267-287. https://doi.org/10.1002/(SICI)1097-0207(20000520)48:2¡267::AID-NME884¿3.0.CO;2-Q

[7] Kara, M., Mesbahi, S., and Angot, P. (2021). The Fictitious Domain Method with Sharp Interface for Elasticity Systems with General Jump Embedded Boundary Conditions. Advances in Applied Mathematics and Mechanics, 13(1), 119-139. https://doi.org/10.4208/aamm.OA-2019-0119

[8] Ramière, I., Angot, P., and Belliard, M. (2007). A fictitious domain approach with spread interface for elliptic problems with general boundary conditions. Computer Methods in Applied Mechanics and Engineering, 196(4-6), 766-781. https://doi.org/10.1016/j.cma.2006.05.012

[9] Ramière, I., Angot, P., and Belliard, M. (2007). A general fictitious domain method with immersed jumps and multilevel nested structured meshes. Journal of Computational Physics, 225(2), 1347-1387. https://doi.org/10.1016/j.jcp.2007.01.026

[1] Laboratory of Applied Mathematics, Department of Mathematics, Faculty of Sciences, Sétif 1 University Ferhat Abbas, Sétif, Algeria.

Email address: ahmedayoub.boukelia@univ-setif.dz

Email address: mohamed.kara@univ-setif.dz